Materials Science in Semiconductor Processing 173 (2024) 108159

Contents lists available at ScienceDirect

Materials Science in Semiconductor Processing

journal homepage: www.elsevier.com/locate/mssp

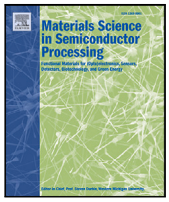

Full length article

Comprehensive analysis of DFT-3C methods with B3LYP and experimental data to model optoelectronic properties of tetracene

Periyasamy Angamuthu Praveen *, Dhanapal Saravanapriya, Sreegowri V Bhat, Kandhasamy Arulkannan, Thangavel Kanagasekaran *

Organic Optoelectronics Laboratory, Department of Physics, Indian Institute of Science Education and Research - Tirupati, Tirupati, India

ARTICLE INFO

Keywords:
Organic semiconductors
Organic Light Emitting Transistors
Tertracene
Reorganization Energy
DFT
Charge transfer
TDDFT
Excited state

ABSTRACT

Modern computational chemistry methods aid experimentalists in scrutinizing molecular systems for organic optoelectronic device fabrication. They are also helpful for device engineering, such as choosing metals for contact fabrication without sophisticated instrumentation. The B3LYP functional with 6-31G(d,p) or 6-311G(d,p) basis set is a widely used method in this regard. Recently, many upgraded methods, such as the three-fold corrected composite scheme (3C), have been reported to offer cost-effectiveness and better accuracy than the B3LYP. This is particularly interesting from a materials engineering point of view as these methods offer the possibility of rapidly screening the materials prior to the experimental analysis. In order to evaluate their suitability towards organic optoelectronic systems, in this work, we have used three composite schemes, namely B97-3C, PBEh-3C and HF-3C, along with B3LYP and the experimental data. The well-studied tetracene system is considered for the analysis, and different optoelectronic properties such as bandgap, reorganization energy, and absorption maximum are calculated theoretically and compared with the experimental data. The results indicate that though slightly expensive, B3LYP performs better than the 3C methods. Of the three, only PBEh-3C performs on par with B3LYP in accuracy and time. A note of caution is that these results should be inferred as this level of theory is adequate for the screening and modeling optoelectronic systems rather than a potential computational chemistry method.

1. Introduction

Organic semiconductors (OSC) are structurally tunable carbon-based materials suitable for fabricating low-cost, flexible optoelectronic devices. Already, the potential of these materials can be perceived from the commercial success of active matrix organic light emitting diodes and the promising results from the photovoltaic systems [1,2]. The OSCs are expected to replace the present silicon-based inorganic optoelectronic devices in the arena, such as the phototransistors, wearable X-ray and bio-sensors, and light-emitting transistors etc [3,4]. Particularly, organic light-emitting transistors (OLET) offer the possibility to combine both control and emission units in a single pixel and are promising systems to develop future flexible and ultra-slim displays [5,6]. Further, the OLETs are considered as the first step towards the realization of long-sought electrically pumped organic lasers [7].

In order to develop an efficient OLET, the active medium (OSC) should have high ambipolar carrier mobility and high photoluminescence quantum yield (PLQY) [8]. However, a material with high mobility and high PLQY is hard to realize due to the inherent limitation of organic systems. The intermolecular $\pi - \pi$ stacking and the high electronic coupling in OSCs induce strong intermolecular charge transport in the system, resulting in high mobility. On the other hand, strong $\pi - \pi$ stacking would lead to the formation of excimers and other nonradiative decay processes resulting in fluorescence quenching [9]. So, in order to develop OLETs, a trade-off between mobility and PLQY has to be established. This necessitates the need for computational aids to simulate the material's properties. In the past, different quantum chemical approaches such as ab initio, semi-empirical and density functional theory (DFT) are employed in this regard [10–12]. Even data-driven approaches have also gained interest recently [13]. Of these, DFT is one of the most widely used methods owing to its robustness and cost-effectiveness compared to its counterparts, such as ab initio and semi-empirical methods. Particularly, empirical and semi-empirical techniques are prone to errors and often require a reliability check. However, the entirely wrong structures or results are very scarce in a DFT calculation. Due to this, many DFT methods are used by non-theoretical experts as black-box methods to study different materials, ranging from metal clusters to proteins.

* Corresponding authors.
E-mail addresses: praveen@iisertirupati.ac.in (P.A. Praveen), kanagasekaran@iiseritupati.ac.in (T. Kanagasekaran).

https://doi.org/10.1016/j.mssp.2024.108159
Received 19 August 2023; Received in revised form 27 November 2023; Accepted 19 January 2024

Among many reported methodologies, DFT with B3LYP functional and with the basis sets 6-31G(d,p) and 6-311G(d,p) is one of the widely used choices for the simulation of optoelectronic materials [14,15]. Specifically, when theoretical aids are employed to assist with the experimental process, these approaches are the major choices to simulate HOMO, LUMO, energy gap, absorption maximum and emission maximum. Such data would contribute to selecting the metal contacts or pumping source for organic field effect transistors or optically pumped lasers [16,17]. On the other hand, computationally, B3LYP, along with 6-31G(d,p), is shown to be less effective and particularly ineffective for modeling non-covalent interactions. So, often, methods like M06-2X, wB97XD or CAM-B3LYP are considered in this regard [18,19]. Recently, there has been a great surge of interest in simplified DFT approaches, termed as 3C methods, shown to have good accuracy with better computational efficiency than the B3LYP [20]. The shorter CPU times with good accuracy are attractive perspectives from an experimentalist point-of-view. They would make more molecules to be tested theoretically, and potential candidates can be chosen for experimental analysis.

Particularly to formulate a prospective OLET design, parameters such as molecular planarity, reorganization energy, charge transport integral, oscillator strength in the excited state(s), radiation lifetime, and transition dipole moments are highly desirable, and based on these parameters, potential candidates can be scrutinized [21]. In the present work, we have chosen a well-known organic semiconductor, tetracene, and studied its structural, electronic and optical properties with B3LYP and three other 3C methods such as HF-3C, PBEh-3C and B97-3C. Four different basis sets are used with each of these functionals, such as the 6-31G(d,p), MINIX, def2-mSVP and def2-mTZVP, respectively. As these functionals are equipped with improvements like a global hybrid functional, generalized gradient approximation and augmented with semi-classical correction potentials, they are expected to produce better results with shorter computational time.

Reported in 2013, HF-3C is the first three-fold corrected composite scheme (3C) [22]. Though it is not a DFT functional, it is highly cost-effective and does not suffer from self-interaction errors in charged systems. With the 3C correction, it is expected to compute structures, vibrational frequencies, and non-covalent interactions satisfactorily. One primary advantage is that due to its simple analytical functions, even a large system like proteins can be studied under this scheme [23]. However, since it follows the standard electron correlation, the Coulomb correlation effects cannot be modeled using this method. PBEh-3C is based on the well-known and robust PBE generalized gradient approximation functional, with 42% of non-local Fock exchange [24]. Due to such a large Fock exchange, PBEh-3C offer better SCF convergence and is very useful for modeling condensed metallic systems. Unlike HF-3C, with the double-zeta basis sets, the bond lengths can be accurately estimated using PBEh-3C [20]. In that series, B97-3C is the latest addition, reported in 2018. It is explicitly parametrized using long-range electron correlation effects [25]. It uses a modified triple-zeta TZVP basis set, which covers the entire periodic table up to Rn. Due to its efficient parameterization and lack of any non-local exchange, it is shown to produce accurate molecular geometries and is often dubbed as an effective replacement for classical B3LYP.

We have systematically used these functionals and studied the optoelectronic properties of the tetracene system. The obtained results were compared with the experimental data and the previous reports. It has been found that B3LYP showed similar or better results than the simplified methods, and its accuracy with slightly high computational cost can be tuned with the choice of basis set. The results obtained are discussed in detail in the following sections.

2. Methodology

Four methods, HF-3C, PBEh-3C, B97-3C and B3LYP, are used in the present work. It is worth noting that the HF-3C is not a DFT functional but a Hartree–Fock method with 3C correction. With a minimal basis set, this method is often considered the choice between DFT and the less accurate semiempirical methods. All the calculations are carried out using either ORCA 4.0 or 4.1 program in a personal machine or a Linux cluster. Other 3C methods, such as r2SCAN-3C and B3LYP-3C, can also be chosen; however, we restrict our analysis to the choice of the ORCA 4 version [26,27]. For 3C methods, their default basis sets, such as MINIX, def2-mSVP, and def2-mTZVP, are used, and for B3LYP, 6-31G(d,p) was used. Other basis sets, such as 6-311G(d,p), cc-PVDZ and LANL2DZ, are also considered to evaluate the effect of basis sets. Excluding HF-3C, for all the other calculations, RIJCOSX approximation with suitable auxiliary basis sets was used to speed up the calculations. After geometry optimization, all the structures were subjected to vibrational analysis and ensured to have no negative frequencies. For excited state calculation, TD-DFT with `orca_asa` program was used, and the absorption and emission frequencies were calculated using the default lineshape correction. The entire process is given as a flowchart in the Supplementary Figure. 2.

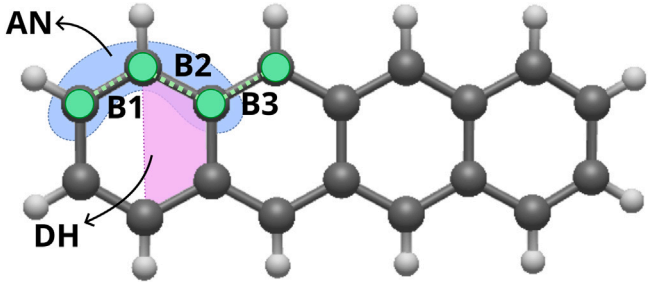

Fig. 1. Molecular structure of tetracene. Colored areas show the selected parameters: B1, B2 and B3 (between green dots) are bond lengths, AN is bond angle (blue region) and DH is dihedral angle (pink region).

In order to compare the spectroscopic properties, commercially purchased tetracene (Merck, 99.999% pure) was used without any further purification. The tetracene single crystals were grown using the physical vapor transport method. The harvested crystals are studied using powder X-ray diffraction analysis (Smart Lab 9 Kw — Rigaku), Fourier-infrared spectroscopy (Bruker ALPHA), UV-vis-absorption spectroscopy (Thermo Scientific, Evolution 201) and fluorescence spectroscopy (JASCO FP-8500).

3. Results and discussion

3.1. Structural properties

In order to compare the structural parameters, we have used the previously reported single crystalline (SC) data of tetracene [28]. To ensure our grown crystals are consistent with the previous report, the sample was powdered and subjected to powder diffraction analysis and compared with the powder pattern generated from the single crystal data. The patterns and the corresponding crystalline parameters are given in the supporting information file (Sec. S1). Similarly, the structural parameters from the optimized geometries, such as bond length, bond angle and dihedral angle, are given in the supporting information file (Supplementary Section. 2), and the selected parameters (Fig. 1) are given in Table 1.

It can be seen that all the methods reproduced the bond lengths and bond angles satisfactorily, and the percentage error is less than 2% compared to SC data (See Supplementary Section 2.5). Though PBEh-3C and B3LYP dihedral angles vary significantly than the SC data, this does not affect the molecular planarity.

In order to gain a better understanding, we have analyzed the molecular planarity using two metrics, molecular planarity parameter (MPP) and span of deviation from the plane (SDP); corresponding

Table 1
Selected bond lengths (B1, B2 and B3) (in Å), bond angle (AN), dihedral angle (DH) (in °), MPP and SDP (arbitrary units) of tetracene for different functionals and basis sets.

Method	B1	B2	B3	AN	DH	MPP	SDP
SC	1.343	1.428	1.385	121.48	0.036	0.0114	0.0425
HF-3C	1.338	1.454	1.372	121.04	0.030	0.0008	0.0032
PBEh-3C	1.356	1.428	1.382	120.95	0.145	0.0021	0.0101
B97-3C	1.362	1.422	1.386	121.05	0.020	0.0003	0.0009
B3LYP	1.367	1.434	1.393	121.10	0.133	0.0044	0.0175

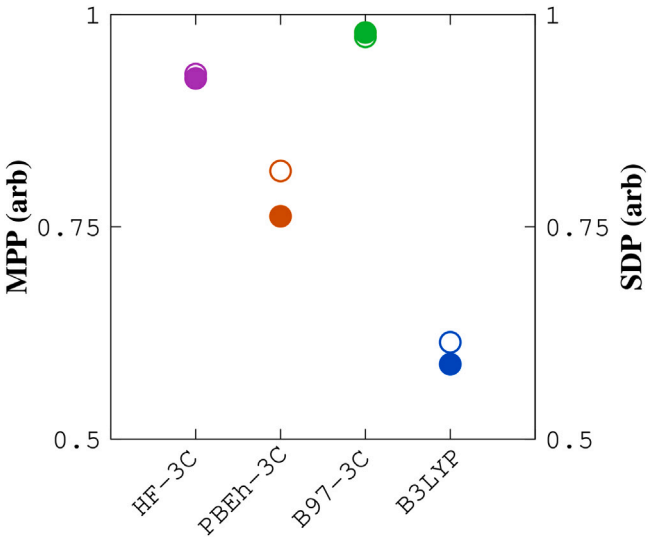

Fig. 2. Percentage difference between SC and DFT simulated values for MPP (filled circles) and SDP (unfilled circles) given in arbitrary (arb) units.

details can be found elsewhere [29]. In short, MPP is a measure of overall deviation in atoms to the fitting plane. In contrast, SDP is a deviation of the molecular span to the fitting plane, and the calculated values are given in Table 1. Since tetracene is a planar molecule, it mostly spans over a single plane, and both MPP and SDP follow a similar trend for all the cases.

The accuracy of molecular planarity indices can be better understood from the percentage difference of MPP and SDP values between the DFT analysis and the SC data. The obtained results are given in Fig. 2. Approaching zero is better, and it can be seen that B3LYP is better than the 3C methods. However, the difference is still twice that of the experimental data, which is a notable factor. In most cases, the slight variation between the MPP and SDP fundamentally arises due to the difference in their fitting planes [29].

The experimental Fourier infrared spectrum of the powdered tetracene single crystal is given in Fig. 3(a). Further, the supporting information file gives the infrared spectrum without any corrections for all the simulated systems (Supplementary Figures. 3–6). B97-3C and B3LYP satisfactorily reproduce the vibrational spectrum. The significant difference between the experimental and theoretical spectrum arises due to the impurities in the sample and the exposure to the atmosphere. Meanwhile, the theoretical spectrum essentially represents the gas-phase spectrum of a single molecule devoid of any solid-state components. In the case of PBEh-3C, the spectrum is more red-shifted. Even the more precise B3LYP method does not perfectly replicate the absorption wavenumbers. A correction parameter is frequently applied to align the theoretical spectrum with the experimental counterpart. For B3LYP and 6-31G(d,p) scheme, 0.96 is a widely accepted value, and with this correction, the resultant spectrum is almost in accordance with the experimental data. To demonstrate the variation in accuracy between different methods, we have taken the single absorption peak located at $\sim$ 460 cm^{-1} in the experimental data and compared it with the simulated data, given in Fig. 3(b). It can be seen that the values vary with respect to the functionals, and underestimating the B97-3C value is nearer to the experimental value followed by B3LYP, PBEh-3C and HF-3C.

3.2. Electronic properties

The energy gap is an important parameter to study in the case of organic optoelectronic systems. Experimentally, the energy gap can be determined from the absorption spectrum using the Tauc plot and the highest unoccupied molecular orbital (HOMO) values from the photoelectron spectrum. The difference between them would yield the lowest occupied molecular orbital (LUMO). Many previous articles have reported these values, and here we refer to this report [30]. The values, along with the simulated values, are given in Table 2.

It can be seen that B3LYP values are better than the 3C methods, and the bandgap values are almost in accordance with the experimental data. Meanwhile, in the case of 3C methods, both B97-3C and PBEh-3C are underperformed, and particularly, HF-3C values are unreliable and do not produce any meaningful insights.

Though it can be argued that B97-3C and PBEh-3C methods resulting reasonable bandgaps, the accuracy of HOMO and LUMO is an essential parameter in the design and fabrication of OLETs. For example, it is a common practice in many experimental papers to use DFT aids (mostly B3LYP with 6-31G (d,p) or 6-311G (d,p)) for the estimation of HOMO, LUMO values. This is due to the fact that the choice of metal contact is based on the metal workfunction and the HOMO and LUMO values of the organic material. Taken the case of tetracene, its HOMO value is −5.3 eV, so Au with work function 5.1 eV can be used for the contacts deposition. Nevertheless, the choices are often limited, and contact engineering approaches like introducing thin layers of metal oxides will be carried out to tune the energy difference. Variations of about or more than $\sim$ 0.2 eV from the simulations would potentially affect this process. So, in such cases, carrying out the experimental characterization rather than lying on the theoretical aids would be the best option.

3.3. Charge transport analysis

Charge transport in organic semiconductors is one of the crucial parameters for OLET systems, and it can be modeled using Marcus theory [31]. In this case, the mobility of the charge carrier is considered to be the hopping process between two molecules. Theoretical predictions often indicate how fast this process is between the molecules in a dimer. Depending on the hole and electron mobility, the OSC can be termed p-type, n-type or ambipolar. In order to derive the hole and electron mobility, two parameters, (a) reorganization energy and (b) charge transfer integral (CTI), are required. These two parameters have to be substituted in a charge transfer rate equation given as,

$$k = \frac{4\pi^2}{h} \frac{J_e^{\pm 2}}{\sqrt{4\pi\lambda^{\pm} k_B T}} exp\left(-\frac{\lambda^{\pm}}{4k_B T}\right) \quad (1)$$

where $\lambda^{\pm}$ is the reorganization energy for hole or electron, $J_e^{\pm}$ is the transfer integral for hole or electron, h is Planck's constant, T is the temperature and k_B is the Boltzmann constant. The CTI indicates the

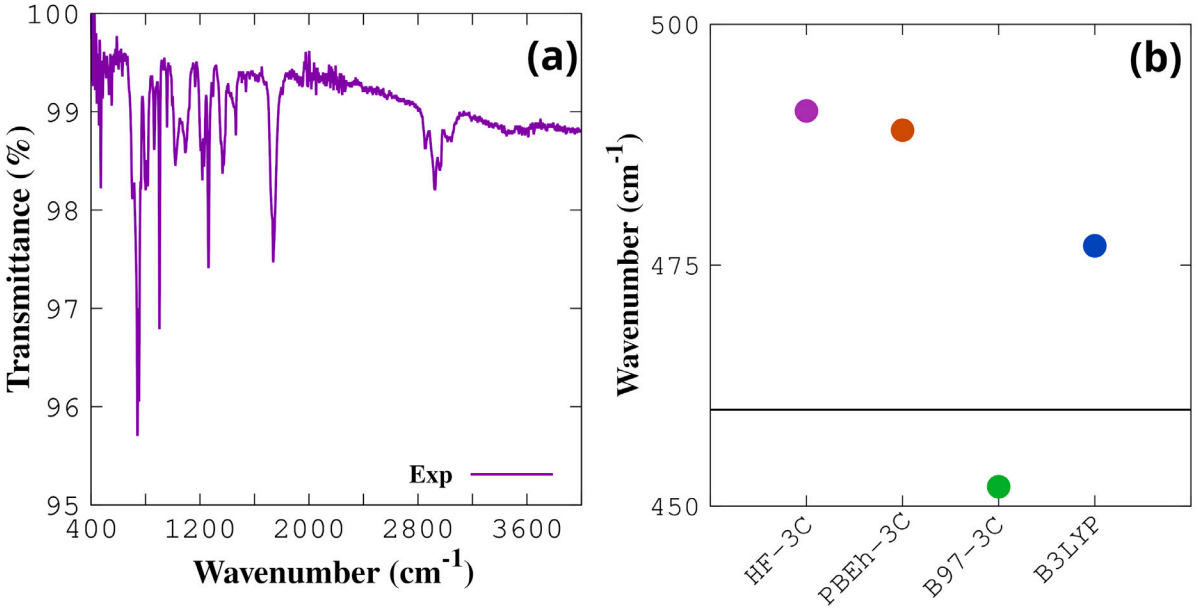

Fig. 3. (a) Fourier infrared spectrum of powdered tetracene single crystals and (b) comparison of experimental peak (~ 460 cm^{-1}) to the DFT spectrum peak. The black line denotes the experimental value.

Table 2
Calculated HOMO, LUMO, E_g (in eV), hole and electron reorganization energies (in meV), IP and EA (in Hartree), abs_{max} (in nm) and f_{osc} (arb) of tetracene.

Method	HOMO	LUMO	Eg	λ^+	λ^-	IP	EA	abs_{max}	f_{osc}
Exp	−5.3	−2.4	2.9	140	–	7.04	0.88	454	0.281
HF-3C	−6.81	1.85	8.66	663.95	704.77	5.68	−0.75	324	0.32
PBEh-3C	−5.88	−1.83	4.05	209.52	163.26	6.70	1.03	462	0.12
B97-3C	−4.50	−2.82	1.68	130.61	81.63	6.37	1.01	562	0.06
B3LYP	−4.76	−1.99	2.77	157.82	111.56	6.18	0.62	498	0.09

interaction strength between the molecules in the dimer. The reorganization energy indicates the energy variation in a molecule due to the structural change when adding or removing the charges. The CTI should be high for better transport, and reorganization energy should be low [21]. One should be cautious while interpreting these theoretical mobility values as they are for dimers and differ greatly from experimental mobility, such as field effect mobility. However, these values could be used to understand the charge transfer trend between different types of molecules. In our previous work, we have substituted furan rings in the place of thiophene and studied the effect of furan based on these mobility trends [11]. The obtained trends indicate which molecule could have better mobility. In order to demonstrate such a trend, in the present case, we have calculated the reorganization energy to understand the functional and basis set effect on charge transfer modeling. The reorganization energy is the sum of inner and outer sphere energies. However, the contribution of outer sphere values is minimal for organic dimers, and often, only the inner sphere energies are calculated. In order to calculate the inner sphere reorganization energy, as per Marcus theory, the energy difference between the neutral and charged state of the molecule is required, as depicted in Fig. 4. It can be given as

$$\lambda^{\pm} = \lambda_1^{\pm} + \lambda_2^{\pm} \tag{2}$$

where ± corresponds to the electron (-) or hole (+) state values and the $\lambda_1^{\pm}$ and $\lambda_2^{\pm}$ values can be directly calculated from the difference in adiabatic potential energy surfaces as,

$$\lambda_1^{\pm} = E_2^{\pm} - E_3^{\pm} \tag{3}$$

$$\lambda_2^{\pm} = E_4^{\pm} - E_1^{\pm} \tag{4}$$

where $E_1^{\pm}$ is the neutral state energy of the optimized geometry, $E_2^{\pm}$ is the energy of the charged state in optimized geometry, $E_3^{\pm}$ is the energy of charged optimized geometry and $E_4^{\pm}$ is the energy of neutral state in charged geometry. The calculated values are given in Table 2, and the energies of neutral and charged states are given in supporting information (Supplementary Section. 4). Experimentally reported p-type reorganization energy is about 140 meV [31]. B97-3C predicts the values near the experimental one, followed by the B3LYP. Here, PBEh-3C overestimates the values, whereas HF-3C values are unreliable. On the other hand, excluding HF-3C, all the functionals indicate a higher electron reorganization energy than the hole, which can be interpreted as the system being more favorable for hole transport than the electrons.

The molecular energies from the neutral and charged state can also be used to estimate the ionization potential (IP) and electron affinity (EA). The values can be calculated using the following relations:

$$IP = E_{cation} - E_{neutral} \tag{5}$$

$$EA = E_{neutral} - E_{cation} \tag{6}$$

These values represent the oxidation and reduction capabilities of the molecule. Notably, in terms of OLET, EA represents the air stability of the molecule, and IP indicates the hole injection in the device [10]. So, in order to estimate and design the device geometry accurately, the DFT functional and basis set combination should yield accurate molecular energies. The calculated IP and EA values are given in Table 2. It can be seen that PBEh-3C predictions are slightly better than the other three functionals, but excluding HF-3C, all the other three functionals produced reasonable values. Though B3LYP underestimates the IP and EA values, its performance can be improved with a better basis set (See Supplementary Section. 6).

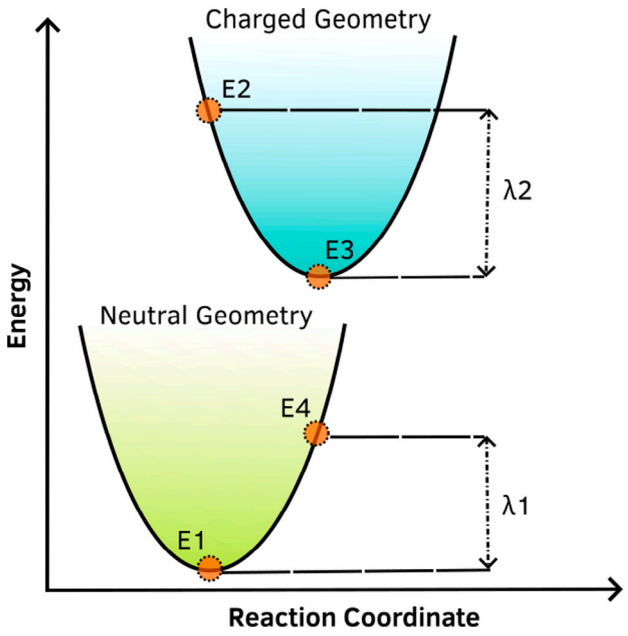

Fig. 4. Marcus diagram for reorganization energy calculation.

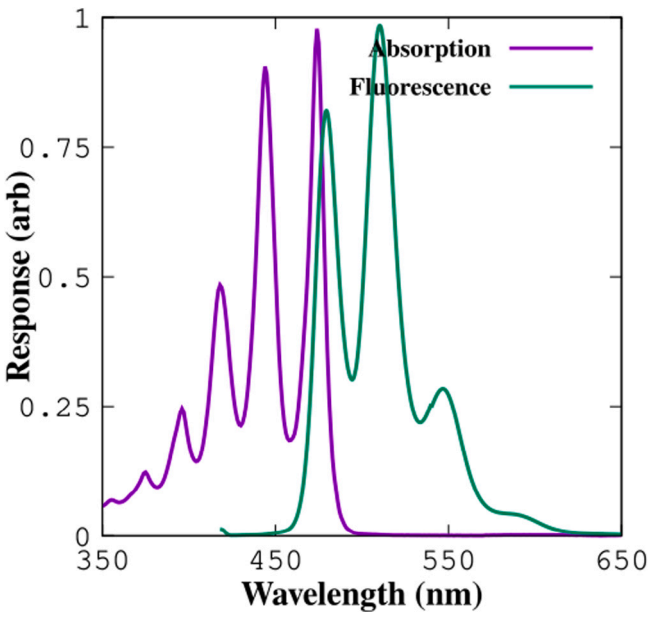

Fig. 5. Recorded absorption and fluorescence spectrum of tetracene single crystals (response is given in arbitrary (arb) units) in THF solution.

3.4. Optical properties

The tetracene single crystals were dissolved in tetrahydrofuran and subjected to absorption and emission studies, and the recorded spectrum is given in Fig. 5. The same spectrum for tetracene molecules with different functionals is given in Fig. 6. Also, the absorption maximum (abs_{max}) and its oscillator strength (f_{osc}) are given in Table 2. It can be seen that PBEh-3C performs better than the other functionals. Also, B3LYP predictions are slightly red-shifted than the actual spectrum. While B97-3C overestimates the spectrum, HF-3C heavily underestimates the excited states, resulting in a poor absorption spectrum. Despite its overestimation (redshift), B97-3C offers the chance to gather the electronic transition features. Meanwhile, HF-3C is highly unreliable in this case too. The variation between experimental data and the data from PBEh-3C and B3LYP is due to the solvation effect. Since `orca_asa` does not have a direct provision to include the solvation effects, we have not discussed those effects here. On the other hand, with the availability of experimental data, `orca_asa` allows the fit of basic functions like Gaussian profile to the theoretical and experimental data so that they can be compared. Such a job is apart from the scope of the present work. Interested can find detailed information in the ORCA manual (Version 4.2.1, Section 9.32). Considering the design of OLET systems, the simulation of absorption and emission spectra plays a crucial role, and the parameters like transition dipole moment and oscillator strengths (f_{osc}) indicate the potentiality of the emissive system. For example, with excitation energy and f_{osc}, the radiative lifetime τ can be calculated [32]. Like transport properties, in this case, slight variation would have a big impact on the prediction of emission wavelength as well as the material's performance. For such high accuracy requirements, a cosmo-based approach or line fitting available in the `orca_asa` can be considered.

3.5. Efficiency analysis

The amount of time the program takes and the accuracy achieved in the results are two crucial queries in any computational chemistry analysis. In order to estimate the efficiency of a method for ground state geometry optimization and excited state calculation, we have used two parameters from our results: (a) bandgap and (b) absorption maximum. The time taken to complete each task is given in seconds. For clarity, the bandgap and absorption maximum values are normalized by dividing them by the experimental value. So, if the values are near one, they can be considered more accurate. So, in a plot, it can be efficient if the time approaches zero and the accuracy approaches one. The obtained plot is given in Fig. 7.

It can be seen that for ground state analysis, PBEh-3C performs very satisfactorily over other functionals. However, it is more expensive and less accurate for the excited state analysis. On the other hand, B3LYP is a bit expensive, particularly for geometry optimization, but it resulted in good accuracy in both cases. It is worth noting that, in many cases, the basis set 6-31G(d,p) produced almost similar results to 6-311G(d,p) with slightly lesser computational time (see Supplementary Sections 6 and 7). On the other hand, these results should not be considered that B3LYP and 6-31G(d,p) is enough, as the performance may vary, particularly for the complex systems when planarity comes into play. B97-3C is often considered a potential choice for fast and efficient DFT analysis. But in the present case, even with the relatively low computational cost, we have observed it is either overestimating (in the case of optical analysis) or underestimating (in the case of electronic analysis) the molecular properties. On the other hand, PBEh-3C is more reliable and produces satisfactory results, of course, with higher computational costs than B97-3C in the case of excited state analysis. So, one can consider B97-3C for initial scrutinization or only if there is a severe limitation in computational power. HF-3C is a choice of functional over semiempirical methods. For example, PM6 and PM7 analysis using MOPAC yields a HOMO of 8.03 eV, LUMO of 1.31 eV and a resultant bandgap of 6.641 eV. The corresponding bond lengths are 1.35, 1.45, and 1.38, with a bond angle 120.91. This does not vary much with the HF-3C results. So, in the present case, though it is a computationally cost-effective system, HF-3C is the least performing and produces no reasonable data. Though expected, we believe this functional has no relevance for the simulation of OLET characteristics.

3.6. Note on choice of basis sets and computational nodes

All three 3C functionals are optimized with the particular basis sets that we discussed. However, ORCA still allows us to use different basis sets. Though it is not recommended, we tried some higher-level basis

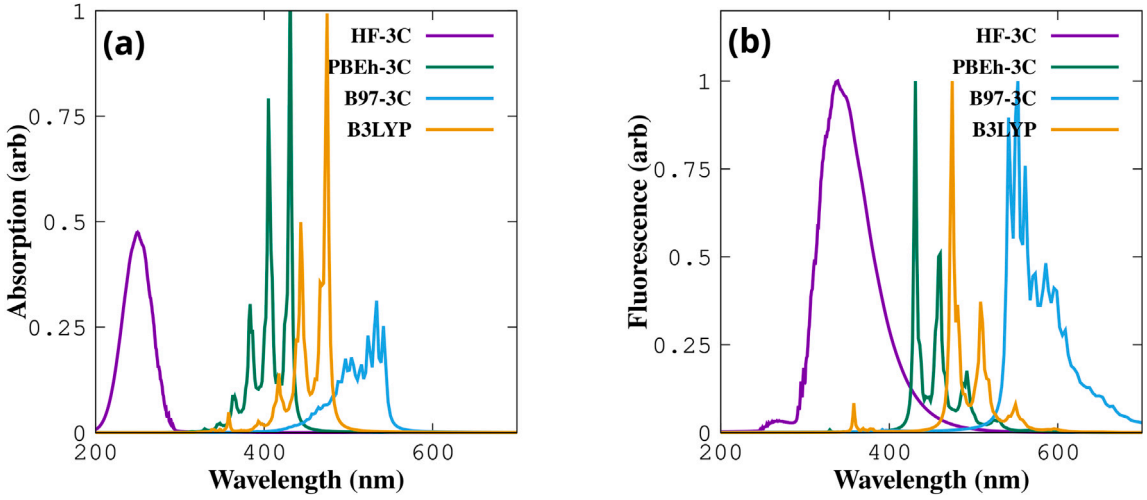

Fig. 6. Simulated (a) absorption and (b) emission spectra for different functionals (response is given in arbitrary (arb) units).

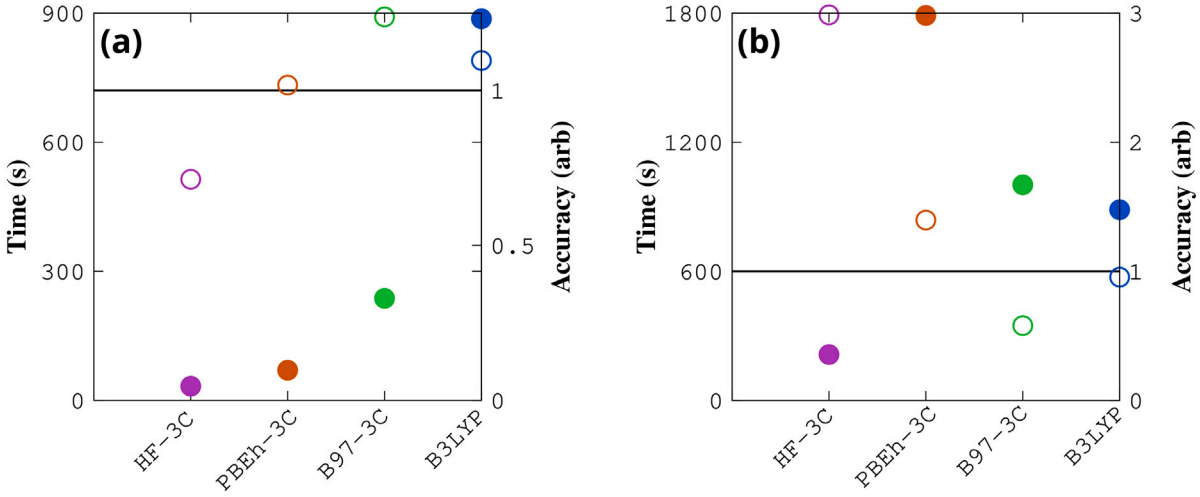

Fig. 7. Computational time (filled circles) and accuracy (unfilled circles — arbitrary (arb) units) of different functionals for (a) bandgap and (b) absorption maximum. Black line indicates the benchmarking value for accuracy.

sets with the 3C functionals. Nevertheless, the accuracy depends mainly on the functional rather than the basis. For example, in the case of HF-3C, using 6-31G, 6-311G, and cc-PVDZ has minimum effect on the frontier orbitals, resulting HOMOs, −4.77, −5.02 and −4.95, LUMOs, −1.99, −2.25 and −2.20 and corresponding bandgap of 2.7 in all cases, respectively. A similar pattern is also observed in the case of other functionals too (given in Supplementary Section. 5).

Further, we have noted a significant difference between running a calculation on a normal personal computer and the high-performance computing nodes (HPC). The HPC would take more time; in some cases, it will be hours compared to the run in a normal system with parallelization. This is due to most of the time the HPC takes to copy the files from the scratch directory to the user directory. Whereas in the case of a normal machine, it is directly written on the current directory, and would fasten if the disk was solid state drive. We have also noted a slight difference in the resulting data in the present case. This is acceptable as our HPC employs an older version (4.0) instead of version 4.1, from which the current results were derived. For example, the final bond angles of B3LYP with 6-31G basis set for the present case are 1.367, 1.434 and 1.393, respectively, differ significantly from the cluster data of the same functional and basis set as 1.367, 1.435 and 1.385. The resultant MPP and SDP of the present case are 0.0044 and 0.0175 against 0.0114 and 0.0425 from the cluster, respectively. There is a slight difference in the excited state calculations, too, for example, an absorption maximum of 498 with an oscillator strength of 0.09 against the 452 and 0.281 for the cluster results. More detailed tables and figures illustrating the results with various basis sets can be found in the supporting information file. (Supplementary Section. 7). We essentially attribute this variation to the difference in ORCA and `orca_asa` versions, and particularly `orca_asa` requires an auxiliary c basis for excited state calculation in ORCA 4.1. This difference can be eliminated when one switches to more recent and effective `orca_esd`, but with significantly higher computational cost.

4. Summary and conclusions

A systematic theoretical approach combined with experimental data is used to evaluate three different simplified functionals and the well-known B3LYP. Different parameters such as bond lengths, bond angles, molecular planarity, vibrational spectrum, molecular orbitals, reorganization energy, ionization potential, electron affinity, absorption and emission spectrum were considered, and each method's performanced is analyzed in terms of OLET characteristics. It has been found that the most widely used B3LYP with 6-31G(d,p) showed a decent performance. In terms of OLET characteristics, all the methods produced good geometry. However, planarity indices are not on par with the experimental data. In particular, the optimal outcomes obtained from B3LYP

are approximately two times lower than the actual data. Similarly, all the methods underperformed in simulating frontier molecular orbitals. In terms of spectral analysis, both B3LYP and PBEh-3C perform very well, and in the case of charge transport analysis, B97-3C yield some good results. It is the only case where B97-3C data is notable. Excluding geometry, the HF-3C resulted in inferior accuracy, and results are on the level of semiempirical data. Overall, with a slightly higher computational cost, B3LYP can be used as a single method for both ground and excited state calculations. On the other hand, PBEh-3C could be a better choice for ground-state analysis. Though it produced good absorption and emission data, the excited state calculations are computationally demanding. We would choose B3LYP with a bigger basis than opt PBEh-3C. There is no reason to use B97-3C, but it can still be considered with limited computational facility. We hope these trends will not vary much for other small organic semiconductors; however, the performances and accuracy may vary with respect to the molecular planarity in complex systems. Further, this investigation focuses on extracting some relevant parameters to aid the device design of OLETs. So, the interpretations in the present case cannot be used (or should be used with caution) in terms of problems like thermochemistry.

CRediT authorship contribution statement

Periyasamy Angamuthu Praveen: Writing – review & editing, Writing – original draft, Visualization, Validation, Software, Project administration, Methodology, Investigation, Formal analysis, Data curation, Conceptualization. **Dhanapal Saravanapriya:** Writing – review & editing, Visualization, Investigation, Data curation. **Sreegowri V Bhat:** Formal analysis, Data curation. **Kandhasamy Arulkannan:** Formal analysis, Data curation. **Thangavel Kanagasekaran:** Writing – review & editing, Writing – original draft, Supervision, Resources, Project administration, Methodology, Investigation, Funding acquisition.

Declaration of competing interest

The authors declare that they have no known competing financial interests or personal relationships that could have appeared to influence the work reported in this paper.

Data availability

All the relevant data is presented within the article and as a supporting information file.

Acknowledgments

This work was supported by SERB CRG grant by Govt. of India (CRG/2022/006100). PP and DS thank the Indian Institute of Science Education and Research - Tirupati for the financial support. KA acknowledges the financial support from University Grants Commission in the form of JRF fellowship (211610111952). SGV thank the Department of Science and Technology, India for the financial support in the form of INSPIRE fellowship (IF210679). The authors acknowledge the support and help from the IT department, IISER-Tirupati for computational facilities.

Appendix A. Supplementary data

Supplementary material related to this article can be found online at https://doi.org/10.1016/j.mssp.2024.108159. Molecular parameters from CIF file, simulated and experimental powder X-ray diffraction patterns, schematic of entire workflow, optimized geometries, percentage difference between single crystal coordinates and optimized geometries, vibrational spectra, neutral and charged state molecular energies, molecular parameter from different basis sets, electronic and optical parameters from different basis sets and time vs accuracy for different functionals and basis sets.

References

[1] J. Song, H. Lee, E.G. Jeong, K.C. Choi, S. Yoo, Organic light-emitting diodes: Pushing toward the limits and beyond, Adv. Mater. 32 (35) (2020) 1907539.
[2] G. Zhang, F.R. Lin, F. Qi, T. Heumuller, A. Distler, H.-J. Egelhaaf, N. Li, P.C. Chow, C.J. Brabec, A.K.-Y. Jen, Renewed prospects for organic photovoltaics, Chem. Rev. 122 (18) (2022) 14180–14274.
[3] J. Kim, S. Song, Y.-H. Kim, S.K. Park, Recent progress of quantum dot-based photonic devices and systems: A comprehensive review of materials, devices, and applications, Small Struct. 2 (3) (2021) 2000024.
[4] G.P. Neupane, W. Ma, T. Yildirim, Y. Tang, L. Zhang, Y. Lu, 2D organic semiconductors, the future of green nanotechnology, Nano Mater. Sci. 1 (4) (2019) 246–259.
[5] Z. Qin, H. Gao, H. Dong, W. Hu, Organic light-emitting transistors entering a new development stage, Adv. Mater. 33 (31) (2021) 2007149.
[6] M.U. Chaudhry, K. Muhieddine, R. Wawrzinek, J. Sobus, K. Tandy, S.-C. Lo, E.B. Namdas, Organic light-emitting transistors: Advances and perspectives, Adv. Funct. Mater. 30 (20) (2020) 1905282.
[7] T. Kanagasekaran, H. Shimotani, K. Kasai, S. Onuki, R.D. Kavthe, R. Kumashiro, N. Hiroshiba, T. Jin, N. Asao, K. Tanigaki, Towards electrically driven organic semiconductor laser with field-effective transistor structure, 2019, arXiv preprint, arXiv:1903.08869.
[8] D. Yuan, V. Sharapov, X. Liu, L. Yu, Design of high-performance organic light-emitting transistors, ACS Omega 5 (1) (2019) 68–74.
[9] Z. Qin, H. Gao, J. Liu, K. Zhou, J. Li, Y. Dang, L. Huang, H. Deng, X. Zhang, H. Dong, High-efficiency single-component organic light-emitting transistors, Adv. Mater. 31 (37) (2019) 1903175.
[10] P.A. Praveen, A. Bhattacharya, T. Kanagasekaran, A DFT study on the electronic and photophysical properties of biphenylyl/thiophene derivatives for organic light emitting transistors, Mater. Today Commun. 25 (2020) 101509.
[11] P.A. Praveen, P. Muthuraja, P. Gopinath, T. Kanagasekaran, Impact of furan substitution on the optoelectronic properties of biphenylyl/thiophene derivatives for light-emitting transistors, J. Phys. Chem. A 126 (4) (2022) 600–607.
[12] R. Jin, X. Zhang, W. Xiao, Theoretical studies of photophysical properties of D-π- A- π- D-type diketopyrrolopyrrole-based molecules for organic light-emitting diodes and organic solar cells, Molecules 25 (3) (2020) 667.
[13] Q. Ou, Q. Peng, Z. Shuai, Computational screen-out strategy for electrically pumped organic laser materials, Nature Commun. 11 (1) (2020) 4485.
[14] G. Gogoi, L. Bhattacharya, S. Rahman, N.S. Sarma, S. Sahu, B.K. Rajbongshi, S. Sharma, New donor-acceptor-donor type of organic semiconductors based on the regioisomers of diketopyrrolopyrroles: A DFT study, Mater. Today Commun. 25 (2020) 101364.
[15] V.S. Puli, M. Subburu, Y. Bhongiri, A. Tripathi, K. Prasad, A. Chatterjee, S. Pola, P. Chetti, New indolo [3, 2-b] indole based small organic molecules for organic thin film transistors (OTFTs): A combined experimental and DFT study, J. Mol. Struct. 1229 (2021) 129491.
[16] K. Oniwa, T. Kanagasekaran, T. Jin, M. Akhtaruzzaman, Y. Yamamoto, H. Tamura, I. Hamada, H. Shimotani, N. Asao, S. Ikeda, Single crystal biphenyl end-capped furan-incorporated oligomers: Influence of unusual packing structure on carrier mobility and luminescence, J. Mater. Chem. C 1 (26) (2013) 4163–4170.
[17] H. Shang, H. Shimotani, T. Kanagasekaran, K. Tanigaki, Separation in the roles of carrier transport and light emission in light-emitting organic transistors with a bilayer configuration, ACS Appl. Mater. Interfaces 11 (22) (2019) 20200–20204.
[18] H. Kruse, L. Goerigk, S. Grimme, Why the standard B3LYP/6-31G* model chemistry should not be used in DFT calculations of molecular thermochemistry: understanding and correcting the problem, J. Organ. Chem. 77 (23) (2012) 10824–10834.
[19] M. Bursch, J.-M. Mewes, A. Hansen, S. Grimme, Best-practice DFT protocols for basic molecular computational chemistry, Angew. Chemie Int. Ed. 61 (42) (2022) e202205735.
[20] E. Caldeweyher, J.G. Brandenburg, Simplified DFT methods for consistent structures and energies of large systems, J. Phys.: Condens. Matter 30 (21) (2018) 213001.
[21] A. Bhattacharya, P.A. Praveen, S.V. Bhat, S. Dhanapal, A. Kandhasamy, T. Kanagasekaran, Theoretical insights on pyrene end-capped thiophenes/furans and their suitability towards optoelectronic applications, Comput. Theoret. Chem. 1225 (2023) 114135.
[22] R. Sure, S. Grimme, Corrected small basis set Hartree-Fock method for large systems, J. Comput. Chem. 34 (19) (2013) 1672–1685.
[23] M. Korth, M. Pitonak, J. Rezac, P. Hobza, A transferable H-bonding correction for semiempirical quantum-chemical methods, J. Chem. Theory Comput. 6 (1) (2010) 344–352.
[24] J.G. Brandenburg, E. Caldeweyher, S. Grimme, Screened exchange hybrid density functional for accurate and efficient structures and interaction energies, Phys. Chem. Chem. Phys. 18 (23) (2016) 15519–15523.
[25] J.G. Brandenburg, C. Bannwarth, A. Hansen, S. Grimme, B97-3c: A revised low-cost variant of the B97-D density functional method, J. Chem. Phys. 148 (6) (2018).

[26] P. Pracht, D.F. Grant, S. Grimme, Comprehensive assessment of GFN tight-binding and composite density functional theory methods for calculating gas-phase infrared spectra, J. Chem. Theory Comput. 16 (11) (2020) 7044–7060.
[27] S. Grimme, A. Hansen, S. Ehlert, J.-M. Mewes, r2SCAN-3c: A "swiss army knife" composite electronic-structure method, J. Chem. Phys. 154 (6) (2021).
[28] D. Holmes, S. Kumaraswamy, A.J. Matzger, K.P.C. Vollhardt, On the nature of nonplanarity in the [N] phenylenes, Chem. Eur. J. 5 (11) (1999) 3399–3412.
[29] T. Lu, Simple, reliable, and universal metrics of molecular planarity, J. Mol. Model. 27 (9) (2021) 263.
[30] J. Sancho-García, A. Pérez-Jiménez, Accurate calculation of transport properties for organic molecular semiconductors with spin-component scaled MP2 and modern density functional theory methods, J. Chem. Phys. 129 (2) (2008).
[31] W.-Q. Deng, W.A. Goddard, Predictions of hole mobilities in oligoacene organic semiconductors from quantum mechanical calculations, J. Phys. Chem. B 108 (25) (2004) 8614–8621.
[32] S. Bibi, F. Farooq, F.Q. Bai, H.-X. Zhang, DFT and TD-DFT studies of phenothiazine based derivatives as fluorescent materials for semiconductor applications, Mater. Sci. Semicond. Process. 134 (2021) 106036.